Pergamon

Cement and Concrete Research 31 (2001) 563–569

CEMENT AND CONCRETE RESEARCH

Speciation of cadmium in cement Part I. Cd^{2+} uptake by C-S-H

Marie-Pierre Pomiès*, Nicolas Lequeux, Philippe Boch

Laboratoire Céramiques et Matériaux Minéraux, Ecole Supérieure de Physique et de Chimie Industrielles, 10 rue Vauquelin, 75005 Paris, France

Received 3 March 2000; accepted 14 November 2000

Abstract

Hazardous cadmium can be trapped in C-S-H, the main "phase" in Portland cement. Two kinds of Cd-containing calcium silicates were synthesized: Cd/Ca silicate hydrates prepared by coprecipitation and Cd-exchanged C-S-H. In Cd-exchanged C-S-H, chemical and structural studies (ICP-AES, XRD, extended X-ray absorption fine structure (EXAFS), and nuclear magnetic resonance (NMR)) show that up to 30 wt.% Cd uptake is possible, with little structural change. XRD patterns and ^{29}Si magic angle spinning (MAS) NMR spectra are similar in Cd-free and Cd-containing C-S-H. Cd-EXAFS shows that the majority of Cd^{2+} atoms are homogeneously distributed within the C-S-H structure, although ^{113}Cd cross-polarization (CP) MAS NMR cannot discriminate between Cd atoms in main layer location and Cd atoms in interlayer location. In Cd/Ca silicate coprecipitates, the structure is nearly amorphous and the silicate species do not polymerize to a C-S-H-like structure.

Keywords: C-S-H; EXAFS; Adsorption; Cadmium; Waste management

1. Introduction

Industrial activities generate wastes. Migration of toxic elements (e.g. heavy metals or radioactive elements) toward the biosphere is a matter of concern. Various materials have been considered to make barriers or to trap hazardous species. Cements are interesting because they are cheap, easy to use, and effective for waste immobilization. Moreover, various pollutants, in particular, heavy metals, can be present in the raw materials that are used in clinker production, or introduced by the fuel combustion during clinkerization. In all cases, one has to avoid pollutant dissemination. Unfortunately, the mechanisms of pollutant immobilization in cementitious materials are imperfectly understood. The immobilization process (often named "solidification–stabilization process") depends on various parameters, such as (i) chemical interactions between pollutant, cement, and additives, or (ii) physical properties, for instance permeability that control outward mobility of pollutants and inward mobility of corrosive species [1,2]. Theoretical and experimental studies are needed on physicochemical speciation (by adsorption, surface complexation, coprecipitation, ion exchange, etc.) of pollutants within cementitious materials.

The two main ways for trapping polluting elements within cements are (i) ionic exchange between already-formed C-S-H and pollutant-containing solutions and (ii) hydration of anhydrous cement using pollutant-containing solutions. This paper (Part I) deals with the first method and the companion paper (Part II) deals with the second one [3].

Many studies have been devoted to the exchange properties of synthetic tobermorite, a mineral that is commonly used for modeling the C-S-H structure [4]. An 11-Å tobermorite substituted with Na^+ and Al^{3+} allows cation exchange with alkalis (Cs^+, Rb^+, and K^+) and alkaline earth elements (the selectivity decreasing from Ba^{2+} and Sr^{2+} to Mg^{2+}) [5–8]. ^{27}Al NMR and ^{29}Si NMR experiments have shown that 15% to 20% Al^{3+} ions can be substituted with Si^{4+} ions inside silicate chains, the positive charge deficit being compensated by the presence of Ca^{2+} or Na^+ ions in the interlayer space [9,10]. Exchange of Na^+ and Ca^{2+} seems facilitated by

* Corresponding author. Tel.: +33-1-40-79-46-34; fax: +33-1-40-79-47-50.

E-mail address: marie-pierre.pomies@espci.fr (M.-P. Pomiès).

0008-8846/00/$ – see front matter
PII: S0008-8846(00)00480-4

the presence of interlayer "cavities" ($\approx$4.7 Å in diameter) due to Si–O–Si bridges between the chains of the main tobermorite layer.

Nonsubstituted tobermorite exhibits cation-exchange properties as well. Shrivastava and Glasser [11,12] and Labhasetwar and Shrivastava [13] have observed exchange of calcium with nickel, cobalt, lead, or magnesium, with no loss of crystallinity. The upper limit of exchanged calcium ($\approx$20%) is close to the interlayer calcium content in tobermorite. Komarneni et al. [14] have found irreversible exchange of Ca^{2+} with Co^{2+} or Ni^{2+} without observable amorphization (for exchange up to $\approx$50% of calcium atoms). They have also reported that Pb^{2+}, Cd^{2+}, Mn^{2+}, Zn^{2+}, and Mg^{2+} do not exchange very much with Ca^{2+}, in which case the exchange sites are located on the surface of tobermorite crystals. An 11-Å tobermorite also shows ion-exchange capacity for Fe^{3+} (up to $\approx$40% of calcium), without loss of crystallinity. ^{57}Fe Mössbauer spectroscopy has shown that the Fe^{3+} ions are located in the Ca^{2+} sites inside the main layer and inside the interlayer of 11-Å tobermorite [15]. Le Callonnec et al. [16] have found that C-S-H materials allow the substitution of large amounts of Fe^{3+} (Fe/Ca = 4) with Ca^{2+}. The Mössbauer spectra of Fe^{3+} exchanged C-S-Hs are similar to those of exchanged tobermorites. Magnetic properties suggest the formation of fine magnetic particles ($\approx$5 nm), whose structure and organization have not been elucidated yet.

Although many data exist on the subject of cation adsorption in tobermorite, little is known on the precise speciation of these ions or on the compounds that are formed (oxyhydroxides, hydroxides, or complexes). Moreover, the exchange capacities of C-S-H, which is the main "phase" in hydrated Portland cement, have not been thoroughly explored. The aim of the present paper is to bring more information on the cadmium uptake in C-S-H-related phases. Cd and Ca exhibit close characteristics. Cd^{2+} is the common valence state of cadmium in aqueous solution, with a ionic radius $\approx$2% smaller than that of Ca^{2+} (0.95 Å for Cd^{2+} and 0.97 Å for Ca^{2+}). Structural isomorphism between Ca and Cd oxides, hydroxides, and silicates is frequent, which suggests the formation of Cd/Ca silicate hydrates.

2. Experimental

2.1. Materials

2.1.1. Cd/Ca silicate hydrates

Cd/Ca silicate hydrates were prepared by a coprecipitation technique. Cd and Ca nitrate mixed solutions were added drop-to-drop to a sodium silicate solution, under a nitrogen atmosphere. The precipitates were washed with deionized water, then dried with acetone and ether. The initial molar ratio (Cd + Ca)/Si was equal to 1 in all samples. The Cd/(Ca + Cd) ratios were 0.12, 0.19, 0.44, and 1. Cd/Ca silicate hydrates were labeled as Series "C".

2.1.2. Cd-exchanged C-S-H

The two series of Cd-exchanged C-S-H were labeled "Ex1" (C/S = 1.28) and "Ex2" (C/S = 0.88). They were prepared by mixing silicic acid and freshly decarbonated CaO in water (water-to-solid mass ratio = 10). The soaking time was 39 days. The C-S-Hs were dried at 35°C in vacuum prior to batch experiments. The cadmium exchange tests were carried out by shaking 250 mg of C-S-H with 100 ml of cadmium nitrate solution (containing from 0 to 2500 ppm of Cd^{2+}) in sealed polyethylene bottles, for 1 month. All experiments were conducted under nitrogen atmosphere, to limit carbonation. The solid was separated from the liquid by Millipore filtration (Cyclopore, 2 μm), then repeatedly washed with deionized water to remove soluble salts, and finally dried with acetone and ether prior to characterization.

2.1.3. Ca/Cd hydroxide solid solutions

Ca/Cd hydroxide solid solutions ($Ca_{1-x}Cd_x(OH)_2$) were prepared to constitute references for NMR and extended X-ray absorption fine structure (EXAFS) studies. The synthesis consisted of dissolving $CaCl_2$ and $CdCl_2$ in water, then mixing with a sodium hydroxide solution. The values of x were 0.03, 0.10, 0.30, 0.50, and 0.70.

2.2. Characterization

Solids and solutions were analyzed by ICP-AES for Ca, Cd, and Si (solids only for Si). Structural characterization was carried out by Cu–K_α XRD (Philips PW1710), ^{29}Si magic angle spinning nuclear magnetic resonance (MAS NMR), ^{113}Cd–^{1}H cross-polarization (CP) MASNMR, and Cd X-ray absorption spectroscopy (XAS).

NMR spectra were recorded using an ASX 500 Bruker spectrometer (spinning at 10 kHz, at the magic angle). ^{29}Si and ^{113}Cd spectra were recorded at 99.36 and 110.94 MHz, respectively, with pulse widths between 4 and 6 μs. For single pulse experiments, the time between pulses was $\approx$120 s, to take into account the long relaxation times of ^{29}Si in C-S-H. For ^{113}Cd CPMAS experiments, the contact time for polarization transfer between ^{1}H and ^{113}Cd was optimized for each sample ($\approx$5 ms). The time between pulses was 10 s. The number of transients collected was typically 1000 to 5000. Chemical shifts were referred to trimethylsilyl-silane (TMS) for ^{29}Si and to cadmium perchlorate hexahydrate ($Cd(ClO_4)_2 \cdot 6H_2O$) for ^{113}Cd.

As experiments at Cd K-edge (26.71 keV) were conducted on the D21 beamline at LURE-DCI synchrotron facility (Orsay, France), using a Si(511) double-crystal monochromator in transmission mode (from 26.55 to 27.8 keV, steps of 2 eV, accumulation time of 6 s) at 77 K. EXAFS data reduction at the Cd–K edge was accomplished using a least square procedure [17]. Experimental phase-shift and amplitude functions for Cd–O and Cd–Cd were

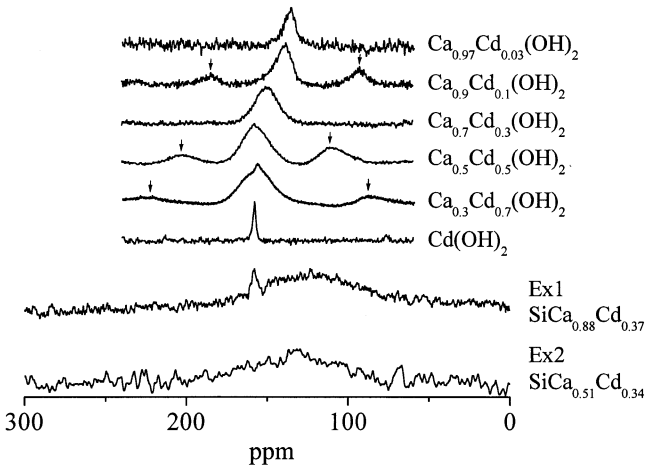

Fig. 1. ^{113}Cd CP MAS NMR of Ca–Cd solid solutions and of 2500 ppm Cd-exchanged C-S-H (Series Ex1 and Ex2). Only the cation contents are indicated. Arrows = spinning side bands.

extracted from the spectra of β-$Cd(OH)_2$ (brucite-like structure). In this structure, a cadmium atom is sixfold coordinated with six oxygen atoms at 2.27 Å and six cadmium atoms at 3.50 Å [18]. Experimental Cd–Ca functions were obtained from $Cd_{0.1}Ca_{0.9}(OH)_2$, which is isostructural to β-$Cd(OH)_2$, as will be explained later on. The low content of cadmium allowed us to neglect the Cd–Cd pair contribution in the cation–cation shell. FEFF-6 theoretical functions [19] were used for Si shells, since we were not able to find any reference material with distinct and isolated Cd–Si shells. The EXAFS functions were Fourier-transformed to obtain a pair distribution function relative to the adsorbing atom. The EXAFS parameters (nature and number of neighbors, radial distance, and Debye–Waller disorder parameter) were then extracted.

3. Results and discussion

3.1. Ca/Cd hydroxide solid solutions

XRD shows that the substitution of Ca by Cd does not greatly modify the structure parameters of portlandite, although there are slight changes in hexagonal cell parameters (a and c). $Ca(OH)_2$ and β-$Cd(OH)_2$ are isostructural and, therefore, the whole solid-solution range experiences variations according to Vegard's law.

The ^{113}Cd CPMAS NMR spectra show the presence of a main line, whatever the Ca/Cd ratio (Fig. 1). In $Cd(OH)_2$, the line is located at 158 ppm and its width is 2 ppm. When the Cd content increases the chemical shift decreases regularly and the line broadens (by 20 ppm). This shows that ^{113}Cd NMR is sensitive to changes of cadmium's next nearest neighbors (be they Cd or Ca atoms). However, the Cd chemical shift when Cd is surrounded by six oxygen atoms in octahedral coordination is at a very different value (-58 ppm instead of 158 ppm) [20], whereas the relatively small range in δ we observed does not indicate a great change in the Cd environment. The line broadening can be due to increased disorder in low-Cd materials. The chemical shift toward high fields as the Cd content decreases is coherent with the slight increase in the Cd–O distance observed by EXAFS (see Table 1).

The transferability of amplitude and phase-shift functions of Cd–O, Cd–Cd, and Cd–Ca pairs extracted from EXAFS data of the end members ($Ca(OH)_2$ and $Cd_{0.1}Ca_{0.9}(OH)_2$)

Table 1
Structural parameters for coprecipitates and Cd-exchanged C-S-H (Series Ex1), as determined by fit of Cd-EXAFS data

	First shell Cd–O			Second shell Cd–Si		Third shell Cd–Cd/Ca			
Samples	d (Å)	Δσ (Å)[a]	N	d (Å)	N	Shell	d (Å)	Δσ (Å)[a]	N
References									
$Cd(OH)_2$	2.27[b]	–	6[b]			Cd–Cd	3.50[b]	–	6[b]
$Cd_{0.1}Ca_{0.9}(OH)_2$	2.29	0.025	5.7			Cd–Ca	3.50[b]	–	6[b]
$Cd_{0.5}Ca_{0.5}(OH)_2$	2.28	0.037	6.0			Cd–Cd	3.50	0.008	2.9
						Cd–Ca	3.50	0.001	3.1
Series C[c]									
$SiCa_{0.88}Cd_{0.12}$	2.24	0.050	4.7	3.30	1.5	Cd–Ca	3.71	0.060	2.6
$SiCa_{0.56}Cd_{0.44}$	2.25	0.057	5.4	2.80	0.5	Cd–Ca	3.69	0.022	3.5
						Cd–Cd	3.69	0.008	0.5
SiCd	2.24	0.060	5.1	3.32	0.7	Cd–Cd	3.42	0.010	0.7
Series Ex1[c]									
$SiCa_{1.15}Cd_{0.08}$	2.24	0.050	5.2			Cd–Ca	3.73	0.061	4.5
$SiCa_{1.05}Cd_{0.14}$	2.26	0.057	5.3	2.89	0.5	Cd–Ca	3.73	0.005	2.3
$SiCa_{0.88}Cd_{0.37}$	2.26	0.061	5.5			Cd–Ca	3.72	0.050	4.1

[a] Difference between fitted and references values of σ for each Cd–X shell.
[b] Fixed values.
[c] The water content has been omitted in the formula.

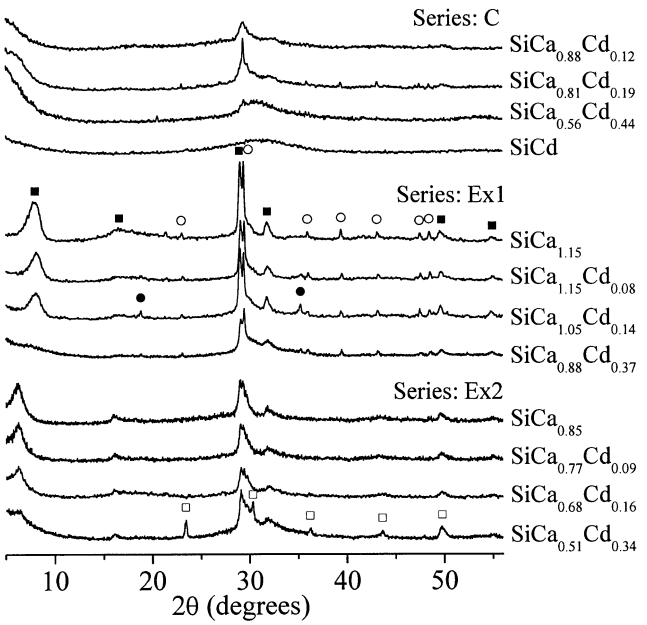

Fig. 2. XRD of coprecipitates (Series C) and of Cd-exchanged C-S-H (Series Ex1 and Ex2). ■ = C-S-H, ○ = $CaCO_3$ (calcite), ● = β-$Cd(OH)_2$, and □ = $CdCo_3$ (otavite).

were tested on the 50:50 solid solution. The fit of the first cation–cation shell (second peak of the radial distribution function) leads to an equal number of Ca and Cd atoms (the total number being of six) located at the same distance of an absorbing atom (see Table 1). A decrease in the Cd content yields an increase in the Debye–Waller factor of the first Cd–O shell, in agreement with the broadening of the ^{113}Cd NMR line.

3.2. Cd-containing precipitated C-S-H (Series C)

XRD data of Cd silicate hydrate is typical of an amorphous material (Fig. 2). As the Ca/Cd ratio increases, the pattern becomes similar to the pattern of poorly crystallized C-S-H, with two main Bragg peaks (at $2\theta \approx 29°$ and 32°).

The amorphous character of Cd silicate hydrate is confirmed by ^{29}Si NMR (Fig. 3 and Table 2), as shown by the wide chemical shift distribution (−65 to −100 ppm), which includes Q^0 to Q^3 species[1]. When the Cd content decreases, one can resolve two distinct lines. The main line is centered at −85 ppm, which is typical of Q^2 species, and the other one is centered at −96 ppm, which is typical of Q^3 species. The Q^2/Q^3 ratio decreases and the Q^3 line disappears when the Cd/(Ca + Cd) ratio becomes inferior to ≈0.1. For this last ratio, one can see a shoulder on the Q^2 line, which can be due to the presence of a few Q^1 species, in agreement with what is expected for Cd-free C-S-H with C/S ≈ 1 [21].

[1] A Q^n species corresponds to a SiO_4^{4-} tetrahedron connected to n similar tetrahedra through oxygen atoms, n being able to vary from 0 to 4.

EXAFS functions and radial distribution functions of coprecipitates are shown in Fig. 4. The fitting procedure results are presented in Table 1. The first peak of the Fourier transform is related to the Cd–O contribution and can be fitted using one oxygen shell only. The Cd–O distance in these silicates is slightly shorter than in Cd hydroxide (≈2.27 Å), and it does not change when the Cd/Ca ratio changes. The mean coordination number is about five, but the strong correlation between Debye–Waller and coordination parameters means this value is not accurate. The typical accuracy of coordination number by EXAFS analysis is about 10%, but it can be worse in the case of large static radial disorder, as observed here. A second peak detected in the Fourier transform is located at ≈3.5 Å (distance not corrected for phase shift). Different fits were tested with either monoatomic or polyatomic shells, for each material. The best results were obtained with a Ca shell at ≈3.70 Å of the absorber for the Cd/Ca silicates. In Cd-rich materials (Cd/Ca ≈ 0.8), one observes a contribution of Cd atoms, but the Cd/Ca ratio deduced from the coordination number is not equal to the stoichiometric ratio. For the Cd silicate precipitates ($SiO_2CdO{\cdot}xH_2O$), the second shell can be fitted with a Cd shell at ≈3.42 Å, which is a distance similar to the Cd–Cd distance in $Cd(OH)_2$ (≈3.48 Å). The low intensity of this peak is typical of a large radial disorder in amorphous materials.

In all cases, one observes an intermediate, low-intensity peak between 2.8 and 3.3 Å in the Fourier transform. In spite of some difficulties to fit this peak, we think it is due to silicon atoms. Ca-EXAFS of Ca silicate minerals have shown that the Ca–Si contributions are difficult to

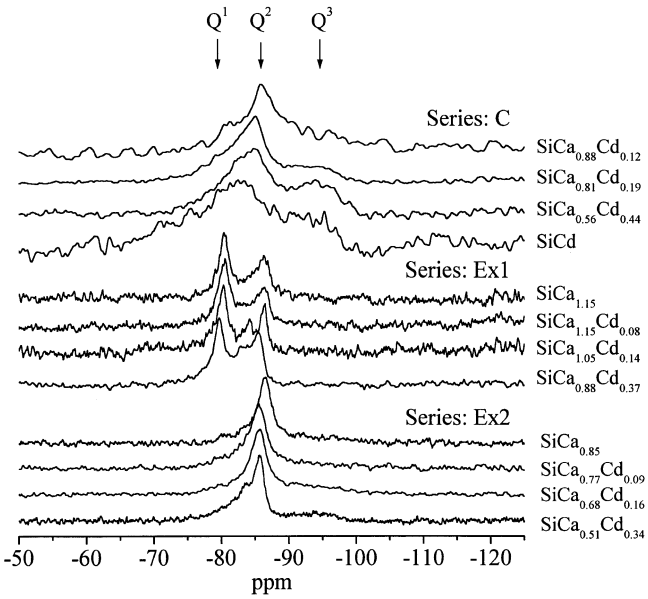

Fig. 3. ^{29}Si MAS NMR of coprecipitates (Series C) and Cd-exchanged C-S-H (Series Ex1 and Ex2).

Table 2
^{29}Si MAS NMR experiments on Series C, Exl, and Ex2

Sample	δQ^1 (ppm)	δQ^2 (ppm)	δQ^3 (ppm)	Mean chain length[a]
Series C				
$SiCa_{0.88}Cd_{0.12}$	− 81.0	− 85.7		
$SiCa_{0.81}Cd_{0.19}$		− 85.4	− 97.3	
$SiCa_{0.56}Cd_{0.44}$		− 85.8	− 96.0	
SiCd			− 70 to − 100	
Series Ex1				
$SiCa_{1.15}$	− 80.4	− 86.0 (− 84.0)		3.8
$SiCa_{1.15}Cd_{0.08}$	− 80.5	− 86.0 (− 84.0)		3.3
$SiCa_{1.05}Cd_{0.14}$	− 80.2	− 86.0 (− 84.0)		3.2
$SiCa_{0.88}Cd_{0.37}$	− 79.7	− 85.5 (− 83.3)		4.3
Series Ex2				
$SiCa_{0.85}$		− 86.0		∞
$SiCa_{1.15}Cd_{0.08}$		− 85.5		∞
$SiCa_{1.05}Cd_{0.14}$		− 85.5		∞
$SiCa_{0.88}Cd_{0.37}$		− 85.6 (− 83.5)	− 95.0	∞

[a] The mean chain length is calculated from the Q^1 and $\sum Q^2$ line areas: $L = 2((\sum Q^2/Q^1) + 1)$.

extract, although the first Ca–Si distances are in general of ≈3 Å [17].

3.3. Cd-exchanged C-S-H

ICP-AES chemical analyses of solutions and solids show full cadmium uptake, up to 2500 ppm (see Table 3). The (Ca + Cd)/Si ratio remains at a constant value during the exchange (≈1.15 and ≈0.85 for C-S-H(Ex1) and C-S-H(Ex2), respectively). Due to the incongruent dissolution of C-S-H, these values are slightly lower than the initial ones (≈1.28 and 0.88, respectively).

The XRD powder patterns of nonexchanged samples are typical of a well ordered C-S-H(I) structure [4] (Fig. 2). The broad basal reflection decreases from ≈14 to ≈11 Å as the Ca/Si ratio increases from 0.85 to 1.15, in agreement with Ref. [4]. The Cd/Ca exchange does not affect the XRD patterns, although one can notice a trend toward amorphization in 2500 ppm materials, where the basal reflection is extinct. In spite of the care taken to avoid carbonation, traces of Ca and Cd carbonates were present in certain samples. Traces of $Cd(OH)_2$ were also present in one sample.

The ^{29}Si NMR spectrum of Cd-free C-S-H (Ex2) exhibits one line (− 86 ppm, Q^2 site), whereas the corresponding spectrum for C-S-H (Ex1) exhibit two lines (− 80 ppm, Q^1 site, and − 86 ppm, Q^2 site). These chemical shifts, together with the average lengths of silicate chains deduced from the Q^1/Q^2 ratio, are characteristic of C-S-Hs with C/S ratios from 0.7 to 1.5 (see Table 2) [22]. In Series Ex1, the average chain is composed of three tetrahedra, whereas in Series Ex2, it is infinite. A shoulder is observed at ≈ − 84 ppm on all spectra. It corresponds to bridging Q^2 species, that is to tetrahedra that share no oxygen atoms with the calcium layers but possess two OH^- groups instead [23].

To summarize, ^{29}Si MAS NMR of Cd-containing C-S-H shows that:

(i) The silicate-chain length keeps a constant value when the Cd content varies.

(ii) There is a broad line at − 95 ppm, which corresponds to a small quantity (about 6%) of Q^3 species, in the high-Cd sample in Series Ex2. This indicates a high degree of polymerization for the C-S-Hs, as observed in the coprecipitates.

(iii) There is a slight displacement of all lines toward the low fields, and a higher discrimination between the two Q^2 lines, as the Cd uptake increases. We have observed the same trend for the chemical shifts of Q^2 lines in $CaSiO_3$ and $CdSiO_3$, both isostructural to para-wollastonite (not presented here). This structure contains silicate *dreierketten* chains, as tobermorite. The Q^2 lines move from − 89.3 and − 87.7 ppm for $CaSiO_3$ to − 83.8 and − 80.2 ppm for $CdSiO_3$. Although the crystallographic structure of $CdSiO_3$ has not been determined, one can think that the differences between the Ca and Cd silicate isomorphic structures are limited to small changes in Si-O-Si angles in *dreierketten* chains, those changes being known to modify chemical shift [24,25].

Fig. 1 shows the ^{113}Cd CP MAS NMR spectra for 2500 ppm Cd-exchanged materials (Series Ex1 and Ex2). There is a broad line at a chemical shift of ≈130 ppm (width ≈50 ppm). There is also a narrow line at a chemical shift of ≈158 ppm in the Ex1 sample, which can be due to traces of cadmium hydroxide, as confirmed by XRD. The broad line represents most of the cadmium ions and indicates that these ions are close to protons. The central chemical shift of the broad line is out of the chemical shifts

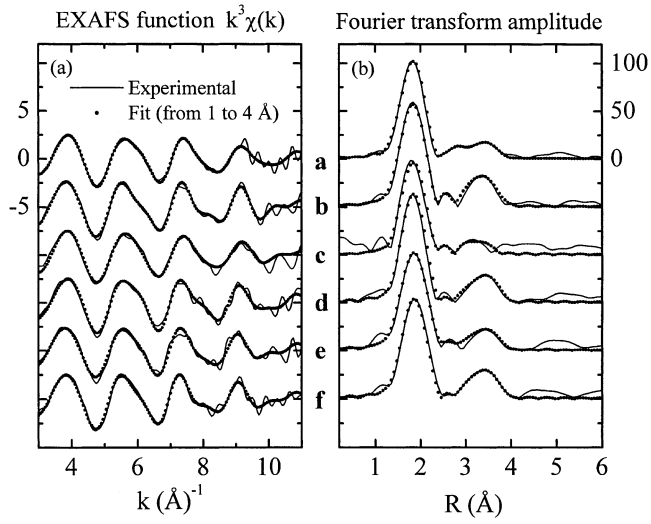

Fig. 4. (a) Cd-EXAFS function and (b) Fourier transform amplitude of EXAFS function. Solid line = experimental data, dots = fit from 0 to 4 Å of the experimental Fourier transform. (a) Series C, $SiCa_{0.88}Cd_{0.12}$; (b) Series C, $SiCa_{0.56}Cd_{0.44}$; (c) Series C, SiCd; (d) Series Ex1, $SiCa_{1.15}Cd_{0.08}$; (e) Series Ex1, $SiCa_{1.05}Cd_{0.14}$; (f) Series Ex1, $SiCa_{0.88}Cd_{0.37}$. Distances observed the Fourier transform are shifted from real distances, due to phase variation with *k*.

Table 3
Chemical analysis of Cd-exchanged C-S-H samples

Series	Initial Cd^{2+} in solution (10^{-3} mol l^{-1})	Ca^{2+} released from C-S-H (10^{-3} mol l^{-1})	Cd^{2+} in solution after equilibrium (10^{-3} mol l^{-1})	Molar ratio in solid (Ca + Cd)/Si	Approximate solid formula[a]
Ex1	0	1.87	–	1.15	$SiCa_{1.15}O_{3.15}$
	4.33	7.67	< 0.01	1.23	$SiCa_{1.15}Cd_{0.08}O_{3.23}$
	8.66	12.20	< 0.01	1.19	$SiCa_{1.05}Cd_{0.14}O_{3.19}$
	21.6	28.10	< 0.01	1.25	$SiCa_{0.88}Cd_{0.37}O_{3.25}$
Ex2	0	2.08	–	0.85	$SiCa_{0.85}O_{2.85}$
	4.33	6.01	< 0.01	0.86	$SiCa_{0.77}Cd_{0.09}O_{2.86}$
	8.66	11.30	< 0.01	0.84	$SiCa_{0.68}Cd_{0.16}O_{2.84}$
	21.6	23.80	< 0.01	0.85	$SiCa_{0.51}Cd_{0.34}O_{2.85}$

[a] The water content is not indicated.

range observed for the solid solutions, which goes from 158 ppm ($Cd(OH)_2$) to 135 ppm (3% Cd solid solution). This line may be the signature of Cd atoms within the C-S-H structure. Using ^{17}O NMR spectroscopy, Cong and Kirkpatrick [26] have shown that Ca–OH sites are always present in the main layer of C-S-H, whatever the C/S ratio. On the other hand, Klur et al. [27] have investigated the structure of ^{43}Ca-enriched C-S-H (C/S = 0.7) using ^{43}Ca NMR. They have found spectra with two peaks. Based on a tobermorite model [28], the first main peak has been assigned to Ca in the main layer and the second one (2% of the total intensity) to hydrated calcium in the interlayer. In the present study, we did not observe the presence of two different Cd sites, as would be expected for a homogeneous distribution of Cd ions in Ca sites. A possible explanation is that the transfer of polarization is more efficient for one kind of sites (main layer or interlayer) than for the other. Another explanation would be that the relative number of occupied interlayer sites is low, for all the exchanged samples we have studied, which means we have principally detected the cadmium atoms in the main layer sites.

EXAFS allows a more accurate description of the Cd environment in Cd-exchanged C-S-H. The structural parameters (Table 1) deduced from EXAFS analysis do not depend on the Cd content. In comparison with the Ca environment in C-S-H [17], the first shell is closer to Cd than it is for Ca (2.26 Å for Cd–O and 2.39 Å for Ca–O). The coordination number is close to six in both cases. The contribution of the Cd–Ca shell at 3.73 Å in Cd-exchanged materials agrees with a tobermorite model with Ca–Ca distances of 3.7–3.9 Å. The Cd-EXAFS spectra do not show any difference in local order around Cd for Cd-exchanged materials and coprecipitates. This means that both samples contain Cd/Ca–O layers, but that the silicate polymerization is different, as indicated by ^{29}Si NMR.

4. Conclusion

1. The Cd–Ca exchange in C-S-H is total for Cd/Ca ratios up to 30 wt.%.

2. The exchange does not induce significant structural changes, although XRD patterns show a tendency to amorphization when the cadmium uptake increases. The ^{29}Si NMR spectra show that the mean silicate chain length does not change when the cadmium content changes. The Cd-EXAFS spectra show a homogeneous distribution of Cd in Ca sites. $^{113}Cd-^{1}H$ CPMAS NMR spectra show one line only, but we cannot discriminate between layer and interlayer sites.

3. The Cd/Ca silicate hydrates prepared by coprecipitation are poorly crystallized. The degree of silicate polymerization is higher than that in C-S-H, although the Cd environment seems identical in coprecipitates and in Cd-exchanged C-S-H.

Acknowledgments

We warmly thank the *Lure* team, especially Robert Cortes, for generous help in EXAFS experiments.

References

[1] D.E. Macphee, F.P. Glasser, Immobilization science of cement systems, MRS Bull. 18 (3) (1993) 66–71.
[2] F.P. Glasser, Chemistry and Microstructure of Solidified Waste Forms, Lewis Publishers, Boca Raton, FL, 1993.
[3] M.-P. Pomies, N. Lequeux, P. Boch, Speciation of cadmium in cement: II. C_3S hydration with Cd^{2+} solution, Cem. Concr. Res. 31 (4) (2001) 571–576.
[4] H.F.W. Taylor, Cement Chemistry, second ed., Thomas Telford, London, 1997.
[5] S. Komarneni, D.M. Roy, R. Roy, Al-substituted tobermorite: Shows cation exchange, Cem. Concr. Res. 12 (1982) 773–780.
[6] S. Komarneni, M. Tsuji, Selective cation exchange in substituted tobermorites, J. Am. Ceram. Soc. 72 (9) (1989) 1668–1674.
[7] M. Tsuji, S. Komarneni, Alkali metal ion exchange and selectivity of Al-substituted tobermorite, J. Mater. Res. 4 (1989) 698–703.
[8] W. Ma, P.W. Brown, S. Komarneni, Sequestration of cesium and strontium by tobermorite synthesized from fly ashes, J. Am. Ceram. Soc. 79 (6) (1996) 1707–1710.
[9] S. Komarneni, R. Roy, D.M. Roy, C.A. Fyfe, G.J. Kennedy, A.A. Bothner-By, J. Dadok, A.S. Chesnick, ^{27}Al and ^{29}Si magic angle spinning nuclear magnetic resonance spectroscopy of Al-substituted tobermorites, J. Mater. Sci. 20 (1985) 4209–4214.

[10] M. Tsuji, S. Komarneni, P. Malla, Substituted tobermorites: ^{27}Al and ^{29}Si MASNMR, cation exchange, and water sorption studies, J. Am. Ceram. Soc. 74 (2) (1991) 274–279.
[11] O.P. Shrivastava, F.P. Glasser, Ion-exchange properties of $Ca_5Si_6O_{18}H_2{\cdot}4H_2O$, J. Mater. Sci. Lett. 4 (1985) 1122–1124.
[12] O.P. Shrivastava, F.P. Glasser, Ion-exchange properties of 11-Å tobermorite, React. Solids 2 (1986) 261–268.
[13] N. Labhasetwar, O.P. Shrivastava, $Ca^{2+} \leftrightarrow Pb^{2+}$ exchange reaction of calcium silicate hydrate: $Ca_5Si_6O_{18}H_2{\cdot}4H_2O$, J. Mater. Sci. 24 (1989) 4359–4362.
[14] S. Komarneni, E. Breval, D.M. Roy, R. Roy, Reactions of some calcium silicates with metal cations, Cem. Concr. Res. 18 (1988) 204–220.
[15] N.K. Labhasetwar, O.P. Shrivastava, Y.Y. Medikov, Mössbauer study on iron-exchanged calcium silicate hydrates: $Ca_{5-x}Fe_xSi_6O_{18}H_2{\cdot}n$-$H_2O$, J. Solid State Chem. 93 (1991) 82–87.
[16] C. Le Callonec, P. Faucon, P. Bonville, N. Genand-Riondet, J.F. Jacquinot, Superparamagnetic properties of a cement derived synthetic Fe substituted calcium silicate hydrate, J. Magn. Magn. Mater. 171 (1–2) (1997) 119–128.
[17] N. Lequeux, A. Morau, S. Philippot, P. Boch, Extended X-ray absorption fine structure investigation of calcium silicate hydrates, J. Am. Ceram. Soc. 82 (5) (1999) 1299–1306.
[18] C. Alétru, G.N. Greaves, G. Sankar, Tracking in detail the synthesis of cadmium oxide from hydroxyl gel using combinations of in situ X-ray absorption fine structure spectroscopy, X-ray diffraction, and small angle X-ray scattering, J. Phys. Chem. B 103 (1999) 4147–4152.
[19] J. Mustre de Leon, J.J. Rehr, S.I. Zabinsky, R.C. Albers, Ab initio curved-wave X-ray absorption fine structure, Phys. Rev. B: Condens. Matter 44 (1991) 4146–4156.
[20] P.G. Mennitt, M.P. Shatlock, V.J. Bartuska, G.E. Maciel, ^{113}Cd NMR studies of solid cadmium (II) complexes, J. Phys. Chem. 85 (1981) 2087–2091.
[21] M. Grutzeck, A. Benesi, B. Fanning, Silicon-29 magic angle spinning nuclear magnetic resonance study of calcium silicate hydrates, J. Am. Ceram. Soc. 72 (4) (1989) 665–668.
[22] X. Cong, R.J. Kirkpatrick, ^{29}Si MAS NMR study of the structure of calcium silicate hydrate, Adv. Cem. Based Mater. 3 (1996) 144–156.
[23] W. Wieker, A.-R. Grimmer, A. Winkler, M. Mägi, M. Tarmak, E. Lippma, Solid-state high-resolution ^{29}Si NMR spectroscopy of synthetic 14 Å, 11 Å, and 9 Å tobermorites, Cem. Concr. Res. 12 (1982) 891–895.
[24] M. Magi, E. Lippmaa, A. Samoson, G. Engelhardt, A.R. Grimmer, Solid-state high-resolution silicon-29 chemical shifts in silicates, J. Phys. Chem. 88 (8) (1984) 1518–1588.
[25] J.V. Smith, C.S. Blackwell, Nuclear magnetic resonance of silica polymorphs, Nature 303 (1983) 223–225.
[26] X. Cong, R.J. Kirkpatrick, ^{17}O MAS NMR investigation of the structure of calcium silicate hydrate gels, J. Am. Ceram. Soc. 79 (6) (1996) 1585–1592.
[27] I. Klur, B. Pollet, J. Virlet, A. Nonat, C-S-H structure evolution with calcium content by multinuclear NMR, in: P. Colombet, A.-R. Zanni, H. Zanni, P. Sozzani (Eds.), Nuclear Magnetic Resonance Spectroscopy of Cement-Based Materials, Springer-Verlag, Berlin, 1998, pp. 119–141.
[28] S.A. Hamid, The crystal structure of the 11 Å natural tobermorite $Ca_{2.25}[Si_3O_{7.5}(OH)_{1.5}]{\cdot}1H_2O$, Zeit Krist. 154 (1981) 189–198.